Null testing toroidal surface and biconic surface with cylinder compensator

Zhuang Liu (刘 壮)[1,2] and Yan Gong (巩 岩)[1*]

[1] *State Key Laboratory of Applied Optics, Changchun Institute of Optics, Fine Mechanics and Physics, Chinese Academy of Sciences, Changchun 130033, China*

[2] *University of Chinese Academy of Sciences, Beijing 100049, China*

[*] *Corresponding author: gongy@sklao.ac.cn*

Received July 11, 2013; accepted August 14, 2013; posted online September 25, 2013

Toroidal surface and biconic surface are employed increasingly, however their profile cannot be null tested easily for they are non-rotationally symmetrical. Null testing method with cylinder compensator is proposed to solve this problem. The theory of this method is revealed. The errors of this method are present. Three typical testing optical systems with cylinder compensator are demonstrated at last. The design results and total error indicate that this method is feasible.

OCIS codes: 220.1000, 220.1250, 220.3620, 220.4840.

doi: 10.3788/COL201311.S22202.

Toroidal surface and biconic surface are increasingly used in modern advanced optical instruments. The toroidal surface which has different radii in sagittal and tangential plane can reduce effectively astigmatism and coma. Thus it is employed widely in off-axis or multi-pass optical system. Biconic surface which has two more degrees of freedom than toroidal surface can improve optical system's performance greatly. They will be widely used in future.

The toroidal surface and biconic surface cannot be tested directly by interferometer without any compensators because they are non-rotationally symmetrical. There are two common methods to test these types of surfaces. One method is use of profilometry. The surface is measured one point or one line at a time by profilometry, profile of the surface can be generated by mapping out several hundred points or lines. This process is not expensive, but it does not offer the detail of an interferometric map. Precision of this method is several tens of nanometers. Accuracy will degrades when table's instability increases due to long distance (in excess of a couple inches). Another option available is null testing with computer generated holograms (CGH), figures can be measured interferometrically. This method is the commonest method, but hologram required the customized program for different surfaces and lithography etching on chrome made it time-consuming, laboring, and expensive. One hologram cannot be used to different profiles[1].

Cylinder surface is also non-rotationally symmetrical. It is curving in one direction and flat in orthogonal directions. As a compensator, cylinder lens can turn the spherical wavefront from one point (the cat-eye) into non-rotationally symmetrical wavefront which fits the tested toroidal surface or biconic surface and take the place of CGH in null testing. Compared with hologram, cylinder lens can be got easily, and one cylinder lens can be used for different profiles.

Methods of null testing toroidal surface and biconic surface with cylinder compensator are discussed in detail. The compensation theory of toroidal surface and biconic surface is shown, and tolerance analysis is covered as well. Three null testing optical systems with cylinder compensator for three typical surfaces are designed. Design results demonstrate this method's feasibility.

The curve of toroidal surface in the tangential plane is defined by

$$Z = \frac{\frac{y^2}{R}}{1+\sqrt{1-\frac{y^2}{R^2}}}. \tag{1}$$

This curve is then rotated about an axis parallel to the Y axis and intersecting the Z axis with a distance ρ from the vertex. Toroidal surface has 2 radii: radius R in sagittal plane and rotate radius ρ in tangential plane. In most cases, the toroidal surface is concave. We set the cylinder lens' generatrix perpendicular to the tangential plane to correct the wavefront from the cat-eye, and discuss its theory in sagittal plane and tangential plane respectively.

In sagittal plane, the cylinder can be considered as a plane plate lens. The plane plate lens whose thickness is not neglected will lead to the longitudinal displacement and wavefront aberration. As a compensator, the primary aberration is 3rd-order spherical wavefront aberration.

As shown in Fig. 1, the longitudinal displacement L produced by passage through a plate of thickness T and refractive index n is easily found by Snell's law for small angle of incidence to be

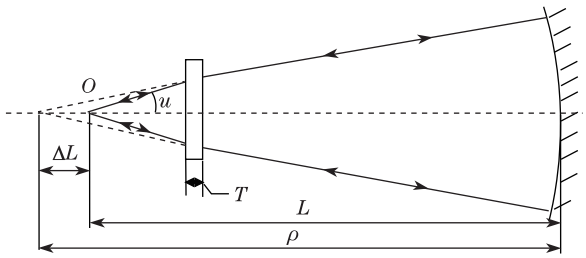

Fig. 1. Layout of compensation optical system in sagittal plane.

$$\Delta L = \frac{(n-1)}{n}T. \tag{2}$$

Then the distance between cat-eye O and the center of toroidal surface is

$$L = \rho - \frac{(n-1)}{n}T. \tag{3}$$

The 3rd-order spherical wavefront aberration with aperture of 1 is given by

$$\Delta W_{\text{sph}} = -\frac{Tu^4(n^2-1)}{8n^3}, \tag{4}$$

where u is the numerical aperture of optical system[2]. Figure 2 gives the graph of ΔW_{sph} for 3rd-order spherical wavefront aberration in wavelength of 632.8 nm, as a function of $2u$, the plate thickness T in millimeters, and refractive index $n = 1.5168$ (N-BK7).

We know from Fig. 2, when $2u \leqslant 1/6$, $T \leqslant 20$, ΔW_{sph} is very small, which can be neglected, otherwise we must set another negative spherical lens or cylinder lens to reduce 3rd-order spherical wavefront aberration.

In tangential plane, L is not equal to the radius R, the cylinder compensator needs at least one spherical surface to change the testing wavefront from the cat-eye to which fits the tangential radius of toroidal surface for astigmatism eliminating. This progress is equal to image the cat-eye O at the center of curvature of tested surface O'. We list three possible optical compensating structures in Fig. 3. Figures 3(a) and (b) are the condition that the difference between R and ρ is small, Fig. 3(a) represents $R > L$, while Fig. 3(b) represents $R < L$, they are equal because we can rotate the system by 90° along the optical axis and exchange the tangential plane and sagittal plane; Fig. 3(c) represents the condition that difference between R and L is great, we cannot compensate it like the way for Figs. 3(a) and (b) because the compensator is very large, so in the plane the radius is small, a converge point is introduced like the way of Offner compensator.

Let the compensating lens be a single thin lens, l be the distance of cat-eyes O to compensating lens, l' be the distance between compensating lens and O', D be the aperture of tested surface in tangential plane. We can get

$$l' - l = R - L. \tag{5}$$

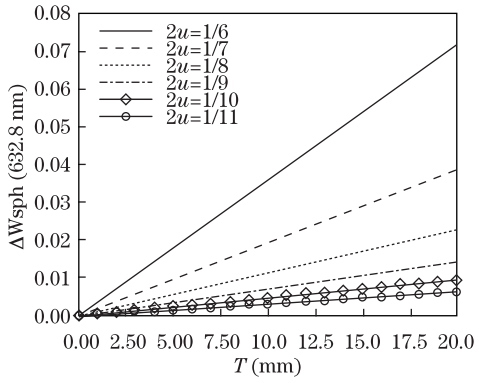

Fig. 2. Third-order spherical wavefront sberration produced by plane plate lens.

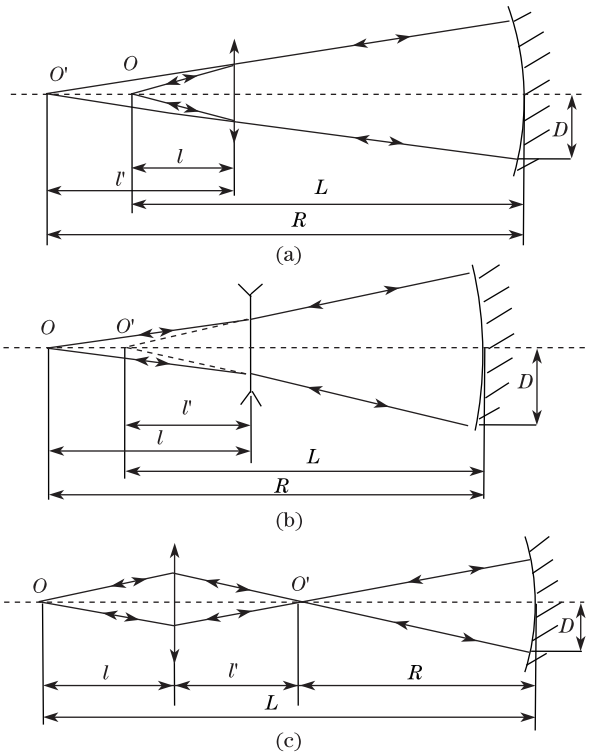

Fig. 3. Layouts of three optical compensating structures in tangential plane. (a) $R > L$; (b) $R < L$; (c) difference between R and L is great.

The 3rd-order spherical aberration produced by a thin lens in imaging progress is

$$W_{\text{sph}} = \frac{h^4\phi^3}{32n}\left\{\left(\frac{n}{n-1}\right)^2 + \frac{(n+2)}{n(n-1)^2}\left[B + \frac{2(n^2-1)}{n+2}C\right]^2 - \frac{n}{n+2}C^2\right\}, \tag{6}$$

where h is the semidiameter of pupil, $h = Dl'/2R$, n is the refractive index of lens, φ is the power of single lens, $\varphi = (n-1)(C_1 + C_2)$, C_1, C_2 are the curvatures of lens' two surfaces. From Eq. (6) and Gaussian Formula, we can get

$$\phi = \frac{1}{l'} - \frac{1}{l} = \frac{l - l'}{l'l} = \frac{L - R}{l'l} \tag{7}$$

the B is the lens shape factor, $B = (C_1 + C_2)/(C_1 - C_2)$, C is the magnification factor, $C = (l' + l)/(l' - l)$.

Then W_{sph} can be expressed as

$$W_{\text{sph}} = \frac{D^4 l'(L-R)^3}{512R^4 l^3 n}\left\{\left(\frac{n}{n-1}\right)^2 + \frac{(n+2)}{n(n-1)^2}\left[\frac{C_1 + C_2}{C_1 - C_2} + \frac{2(n^2-1)}{n+2}\cdot\frac{l'+l}{l'-l}\right]^2 - \frac{n}{n+2}\left(\frac{l'+l}{l'-l}\right)^2\right\}. \tag{8}$$

For a toroidal surface, R, ρ, and D are constant, L does not vary greatly. Therefore spherical aberration of single lens is the function of l, l', C_1, C_2, and n. At the same

time, they must follow the relation:

$$\phi = (n-1)(C_1 - C_2) + \frac{n-1}{n} T C_1 C_2 = \frac{L-R}{l'l}. \quad (9)$$

We can find the best optical system parameters to minimize $W_{\rm sph}$ by optimizing these variables (l, l', C_1, C_2 and n). In most cases, D/R is not great, R and ρ are approximately equal, so l and l' are also approximately equal according to Eqs. (3) and (5). From Eqs. (6) and (7), we can obtain that in tangential plane, the most influential 3rd-order spherical aberration produced by a thin lens will be extremely tiny, thus we can use one compensator in hand to compensate tested toroidal surfaces with different parameters, its feasibility will be demonstrated below. This is a significant advantage of cylinder compensator.

On the other hand, if the difference between R and ρ or D/R is too big, the optimal result may be unacceptable, then a pair of compensating lenses with opposite signs are needed. Obviously, compensator with two or more lenses will play a better role than compensator with single lens, however more lenses means more cost, and more errors introduced by fabrication and alignment.

The biconic surface is defined by

$$z = \frac{\frac{x^2}{R_x} + \frac{y^2}{R_y}}{1 + \sqrt{1 - \frac{(1+k_x)x^2}{R_x^2} - \frac{(1+k_y)y^2}{R_y^2}}}. \quad (10)$$

It has four parameters: R_x, k_x, R_y, and k_y. The elliptical surface which has three degrees of freedom can also be presentd by Eq. (10). As shown in Eq. (10), both curves of biconic surface in tangential and sagittal plane are aspherical, hence we cannot deal with it using the same way of testing toroidal surface. There have been methods of null testing aspheric surface like Offner compensation and Shafer compensation right now. We can employ two or more cylinder lenses perpendicular to each other to compensate the non-rotationally symmetrical wavefront. The total Seidel coefficient for 3rd-order spherical aberration in every plane is

$$S_{\rm I} = S_{\rm I}^M + 2S_{\rm I}^{\rm plane1} + 2S_{\rm I}^{\rm com1} + 2S_{\rm I}^{\rm plane2} + 2S_{\rm I}^{\rm field2}, \quad (11)$$

where $S_{\rm I}^M$, $S_{\rm I}^{\rm plane1}$, $S_{\rm I}^{\rm com1}$, $S_{\rm I}^{\rm plane2}$, and $S_{\rm I}^{\rm field2}$ are the Seidel coefficients for 3rd-order spherical aberration in the tested surface, compensating lens, and field lens, respectively. In order to get good effect, we need $S_{\rm I}$ close to 0 in both sagittal and tangential plane. Undoubtedly, four compensators will produce a lot of troubles in the process of fabrication and alignment, so that we discard two field lenses can get good result as well.

Errors of the null testing aspheric surface with compensator has been discussed[3]. We quote some results and classify them into the interferometer error, environment disturbance error, plane surface irregularity error, cylinder surface irregularity, and the error of optical system design and alignment. The error of optical system design and alignment are different since the optical systems are various. Detail parameters of previous four errors have been listed in Table 1. Tolerances of fabrication and alignment are listed in Table 2. The error created by tolerances of fabrication and alignment can only be calculated for every design.

We know that high-precision cylinder surface is difficult to test and fabricate, the radius tolerance is not smaller than ±0.5 fringes, but fortunately in the progress of testing, removing the compensating lens and the tested surface is feasible, so we can set the thickness between cat-eyes and compensating lens and the thickness between compensation lens and tested surface as compensator when we analyze the tolerances using optical design software.

The total error can be calculated by

$$\delta_{\rm total} = \sqrt{\sum_{i=1}^{N} \delta_i^2} \ (N \text{ is the quantity of errors}). \quad (12)$$

In order to demonstrate the method's feasibility, testing optical systems for three typical surfaces have been designed using optical design software, and the results have been presentd and analyzed.

The first testing system is for a toroidal surface whose radius and rotate radius are approximately equal, the surface's parameter is from the toroidal substrate of extreme-ultraviolet imaging spectrometer's (EIS) grating for Japanese satellite Solar-B. The radius and rotate radius are 1182.873 and 1178.097 mm, respectively, and the aperture of the surface is 90 mm[4]. The D/R and the difference between radius and rotate radius are small, so the aberration created by cylinder lens is small, it

Table 1. Error of Null Testing

Errors	Error Value (RMS, λ=632.8 nm)
Interferometer Elements Error	$\lambda/500^*$
Environment Disturbance Error	$\lambda/500^*$
Plane Surface Irregularity	$\sqrt{2}(n-1)\lambda/80^{**}$
Cylinder Surface Irregularity	$\sqrt{2}(n-1)\lambda/40^{**}$

*Interferometer elements' error and environment disturbance error are different for different interferometer and testing environment;

**Testing optical beam is through compensator's surface twice.

Table 2. Tolerances of Fabrication and Alignment

Cylinder Surface Radius	Surface Thickness	Surface Tilt	Surface Decenter	Surface spherical and Astigmatism Irregularity	Elements Decenter	Elements Tilt	Index Tolerances
±0.5 fringes	±0.005 mm	±5 arc sec	±0.01 mm	±0.2 fringes	±0.01 mm	±5 arc sec	$\pm 10^{-6}$*

*The glass is *N-BK7* of Schott.

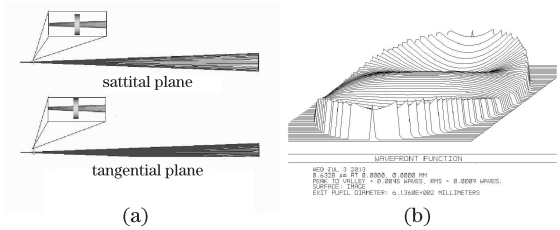

(a) (b)

Fig. 4. Design result of first testing optical system. (a) 3D layout in tangential plane and sagittal plane; (b) wavefront map in (0°, 0°).

Table 3. Detail Parameters of Testing Optical System

Parameter (mm)	System 1	System 2	System 3
Air Thickness 1(d_1)	61.896	292.755	44.655
Glass Thickness 1(d_2)	5.000	10	9.047
Air Thickness 2(d_3)	1113.089	19.966	4.967
Glass Thickness 2(d_4)	——	10	5.623
Air Thickness 3(d_5)	——	674.083	355.018
Radius 1(R_1)	∞	61.683	∞
Rotate Radius 1(ρ_1)	–500	∞	27.326
Radius 2(R_2)	——	34.847	∞
Rotate Radius 2(ρ_2)	——	∞	26.250
Radius 3(R_3)	——	52.25	–22.106
Rotate Radius 3(ρ_3)	——	∞	∞
Radius 4(R_4)	——	–129.470	53.155
Rotate Radius 4(ρ_4)	——	∞	∞

provide a chance to simplify compensator to reduce the compensator's fabrication error and the alignment error. We built a optical system with one plane-convex cylinder lens whose radius is 500 mm, thickness is 5 mm, a satisfactory result is got after optimizing. The final parameter is shown in Table 3 (system 1), and three-dimensions (3D) layout in tangential plane and sagittal plane, the wavefront map in (0°, 0°) of the testing optical system before adding tolerance is shown in Fig. 4. We calculated the RMS wavefront employ Monte Carlo Analysis after adding the tolerance list in Table 2, the RMS wavefront is 90%<0.0390λ, 80%<0.0360λ. Add the other errors list in Table 1, the total error δ_{total}=0.0441λ. After that we change the radius of plane-convex cylinder lens to 200, 300, 1000 mm, equivalent result has been got. Suppose we have a plane-convex cylinder lens whose radius is 500 mm, thickness is 5 mm, and use it to compensate toroidal surface in Refs. [5] and [6], their radius, rotate radius, aperture are (1192.092, 1189.814, 80 mm) and (150.000, 149.520, 24 mm), respectively. After design and calculation, the total errors are δ_{total}=0.0424λ and δ_{total}=0.0432λ, respectively. From the results, we can conclude that cylinder compensator is effective in the null testing for toroidal surface likes the substrate of EIS. We have many choices in cylinder compensator's radius. At the same time, one cylinder compensator can be employed for more than one surface.

The second system is for toroidal surface shown in Fig. 3(c), the radius and rotate radius are supposed to be 500 and 1000 mm, respectively. The aperture is 110 mm. The minimal creative aberration by one cylinder lens cannot be accepted in this example, so a pair of cylinder lenses include a positive lens and a negative lens is adopted. After optimizing, the final parameter is shown in Table 3. 3D layout in tangential plane and sagittal plane and the wavefront map in (0°, 0°) of the testing optical system before adding tolerance is shown in Fig. 5. The RMS wavefront after adding the tolerance is 90%<0.0350λ, 80%<0.0330λ, and the total error δ_{total}=0.0507λ. From the simulation result, we can conclude that cylinder compensator is also effective as the toroidal surface for the case in Fig. 3(c).

The third testing system is for a biconic surface whose parameters is from a mirror of infrared multi-object spectrometer (IRMOS). Detail parameters are: R_x = 407 mm, k_x = 0.127, R_y = 377 mm, k_y = 0.787, aperture: 94 × 76 (mm)[1]. We set up one cylinder surface in both sagittal and tangential plane and achieve wonderful compensation effect after optimizition. The final 3D layout in tangential plane, sagittal plane, and the wavefront map in (0°, 0°) of the testing optical system before adding tolerance are shown in Fig. 6. The RMS wavefront after adding the tolerance is 90%<0.0125λ, 80%<0.0100λ, and the total error is δ_{total}=0.0387λ. From the simulation result, we can conclude that although we use just two compensation lens and discard the field lens, method of cylinder compensator is also efficient to the biconic surface.

Optical system design results of three typical surfaces have demonstrated the feasibility of null testing toroidal surface and biconic surface with cylinder compensator. Now there are still two obstacles as we know for the cylinder compensator's widely popularity. One is the hard-fabrication and low-regularity of high-precision cylinder surface, however, fabricating and testing technology definitely improve because the requirement increases; the other is the time-consuming of testing optical system's alignment, more advanced alignment technology is applied to this testing optical system. In this letter, we only discuss the most common concave tested surface,

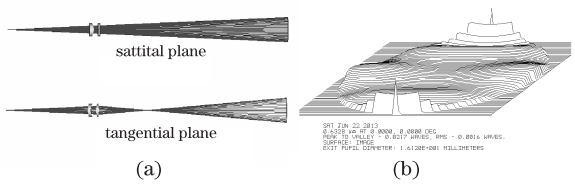

(a) (b)

Fig. 5. Design result of second testing optical system. (a) 3D layout in tangential plane and sagittal plane; (b) wavefront map in (0°, 0°).

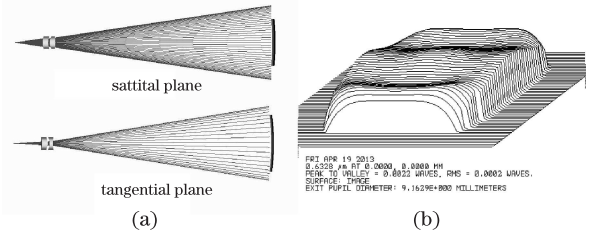

(a) (b)

Fig. 6. Design result of third testing optical system. (a) 3D layout in tangential plane and sagittal plane; (b) wavefront map in (0°, 0°).

further research for the surface like convex or saddle-shaped will be carried out in the future.

This work was supported by the National Natural Science Foundation of China (Nos. 40974110, and 41104122), and White Russian International Cooperation Projection (No. 2011DFR10010).

References

1. V. J. Chambers, R. G. Minka, and R. G. Ohla, Moorwood, Editors, Pro. SPIE **4841,** 689(2003).
2. D. Malacara, *Optical Shop Testing*, (Wiley-Interscience A John Wiley & Sons, Inc, New Jersey, 2007).
3. Z. Zhang and J. Yu, Opt. Pre. Eng. **7,** 1 (1999).
4. C. M. Korendyke, C. M. Brown, and R. J. Thomas, Appl. Opt. **45,** 34 (2006).
5. Z. Liu and Y. Gong, Spectrosc. Spect. Anal. **32,** 3 (1012).
6. L. Yu, S. Wang, Y. Qu, and G. Lin, Appl. Opt. **50,** 22 (2011).